NEW ZEALAND SOCIETY FOR EARTHQUAKE ENGINEERING

The efficacy of damper subsystem stiffness of Linear viscous damper on response reduction in SDOF system.

H.S. Ahmed, S. Beskhyroun & V. Vishnupriya *

Auckland University of Technology, Auckland, New Zealand

*Massey University, Auckland, New Zealand

G. Rodgers

University of Canterbury, Christchurch, New Zealand

ABSTRACT

Recent years have witnessed substantial progress in implementing viscous dampers to mitigate extensive structural responses in high seismic regions. The infinite rigid damper subsystem stiffness has been suggested in practical design due to the challenge of numerically computing its ratio relative to the lateral stiffness of structures. Further analytical examination is performed to calculate the optimal ratio of damper subsystem stiffness to inherent stiffness in the SDOF system, aiming to identify ratios that effectively function as a semi-rigid subsystem and avoid brace flexibility. The study examines various subsystem stiffness ratios, from extremely flexible to semi-rigid, inside the SDOF system under seismic ground motion datasets. A linear viscous damper integrated into the SDOF system is simulated in OpenSEES to determine its optimal stiffness ratio. The study's findings indicated that a stiffness ratio of more than three reduces the SDOF system's structural responses nearly identical to the rigid subsystem. The stiffness of the very flexible damper subsystem exhibits out-of-phase behaviour when the ratio is lower than three.

Keywords: Viscous damper, Subsystem stiffness, Structural response, SDOF system, Brace flexibility

1 INTRODUCTION

Several conventional earthquake-resistant strategies, such as moment-resisting, shear-resisting, braced, and dual frames, are proposed to improve the seismic performance of structures subjected to earthquakes. These strategies rely on the strength and ductility of structural components to withstand the transmitted loads from seismic energy (NEHRP, 2001; Sabelli, 2001). Further, introducing structural configurations such as buckling restrained braced (BRB) can effectively mitigate the dynamic response of structures during earthquakes (Faruk et al., 2023; Silwal et al., 2015). Although earthquake-resistant structures offer greater stability and strength, they do not lack limitations and challenges when properly maintaining the elastic ranges in the event of major quakes. The challenges associated with accommodating large sections of structural components could cause problems in terms of construction cost, aesthetics, constructability, and overloading the foundation (Symans et al., 2008). Hence, an alternate technique becomes crucial for structures beyond the elastic range in regions prone to high seismic events (Losanno et al., 2017). Among the variety of energy dissipation devices, viscous dampers have emerged as a critical answer to the issues of excessive seismic energy that cannot be overcome by the earthquake-resistant structures abovementioned (Abdi et al., 2016; Liu et al., 2023; Mcnamara & Taylor, 2003). These outstanding technologies work by absorbing and changing seismic energy into heat, thereby protecting a building's structural integrity (Kim et al., 2003; Oinam et al., 2014; Seo et al., 2014). Numerous real-world applications have demonstrated the efficacy of viscous dampers in seismic energy dissipation (Infanti et al., 2008). Analytical investigations offer a theoretical foundation for understanding the behaviour of structures equipped with viscous dampers in the form of mathematical models and computer simulations (Hejazi et al., 2014; Mansoori & Moghadam, 2009; Patel & Jangid, 2014). These analytical tools enable researchers to analyse the dynamic response of buildings subjected to seismic force*s*. Researchers also conducted numerous investigations in laboratory settings to investigate viscous dampers' improved characteristics, aiming to dissipate more energy and reduce structural responses (Liu et al., 2023; Zhang et al., 2023)). The results of these experiments not only support the theoretical concepts but show how dampers and other structural components interact. For example, viscous dampers work optimally when installed in the bracing systems; together, the innovative brace-damper configuration reduces structural responses ((Feng et al., 2021; ZHU et al., 2019). Pourzangbar et al. (2020) conducted numerical simulations on the effect of different configurations and damper-brace stiffness on the performance of steel structures, and they found that they achieved effective energy dissipation and structural response control by proposing optimal brace-damper stiffness. A recent study was conducted by (Xie et al., 2022) to investigate the effects of a damper subsystem on reducing structural responses in SDOF systems. The previous research is extended and focuses on SDOF systems characterised by natural periods spanning from 0.25 to 3 seconds. A collection of ground motions derived from the seismic activity of the Christchurch earthquake is employed. The findings of their numerical investigation were that the optimal amount of damper subsystem stiffness should be five times higher than the inherent system stiffness. A more concise understanding of this concept is required to investigate the damper subsystem's exact amount of stiffness ratio to investigate the limit between in-phasing and out-of-phasing behaviour. Determining response reductions in the SDOF system's longer natural period is also worthwhile, as comparing the response reductions for different earthquake actions. Expanding upon previous research, the present study investigates the subject matter by examining longer natural periods (specifically, Tn = 4 seconds) representing high-rise buildings.

A deeper understanding of the effect of damper subsystem stiffness is required to be followed in designing structures equipped with viscous dampers to enhance the seismic performance of the buildings subjected to major earthquakes. Several works are still required to understand the brace flexibility and rigidity of subsystems during design procedures. The analytical investigation was carried out for the purpose of determining the optimised ratio of subsystem stiffness as functional as rigid subsystem and ratios that cause out-of-phase behaviour.

2 NUMERICAL INVESTIGATION

2.1 Effect of Sub-System Stiffness on the Structural Damped Frequency

It is a preliminary investigation to find the effect of brace flexibility on the damped circular frequency. the system is an SDOF comprised of linear spring Ks and viscous dashpot Ci and the system is equipped with a viscous damper subsystem including the linear spring Kd=SR*Ks and dashpot Cd. The latter is found in equation (1) where the damping ratio of the viscous damper. ζ_d ranges from 0.0% to 30% with a 0.6% increment, then to find the value of the damping coefficient of viscous damper Cd.

$$C_d = 2.0\, M.\omega_n\, \zeta_d. \tag{1}$$

where C_d = damping coefficient of the damper; M = mass of the system; ω_n = damped circular frequency; and ζ_d = damping ratio of a viscous damper.

The SDOF system has two nodes (node one is fixed, and node two is free to move and has lumped mass) and three zero elements between nodes representing spring (inherent stiffness), dashpot (inherent damping coefficient), and supplemental dampers including subsystem stiffness Kd and viscous dashpot in series Cd. In OpenSEES, a 1-second rectangular pulse excitation oscillates the system then released to freely vibrate for 19 seconds to establish a 20-second time history. Five stiffness ratios are proposed for each period for the SDOF system's two natural periods, T=1.0 and 2.0 seconds. The designed damping coefficient of the viscous damper for each stiffness ratio was divided into 50 to estimate the damped frequency and damped period from the results of Equation (2).

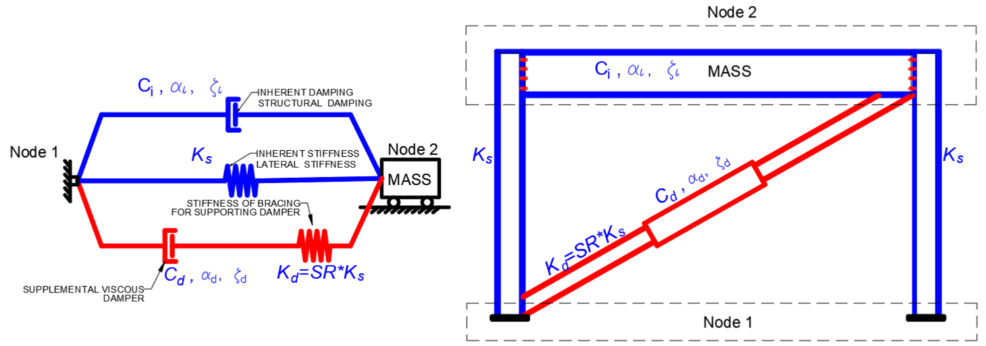

Figure 1: a) Schematic of SDOF system b) One-bay, one-floor frame with supplementary damper

$$\omega_d = \omega_n \sqrt{1 - \zeta_t} \tag{2}$$

where ω_d = damped circular frequency; ω_n = damped circular frequency; and ζ_t = total designed damping ratio, which is the sum of 5% of the inherent damping ratio and the damping ratio of the damper ranging from 0.0% to 30% by 0.6% increment. After calculating the time history displacement, the damped time (Td) is derived by computing the time between two zero crossings. Sixty values of the damped frequency for each stiffness ratio are calculated by using Equation (3). The derived analytical outcome is incorporated into graphs to compare it with various stiffness ratios.

$$\omega_d = \omega_n * T/T_d \tag{3}$$

The following observations were gathered from the data illustrated in Figures 2 and 3. The damped frequency exceeds the natural frequency by 20% when the stiffness ratio varies from 0 to 3. For example, the damped frequency is around 20% more than the natural frequency when the stiffness of the damper subsystem is around 70% of its inherent stiffness.

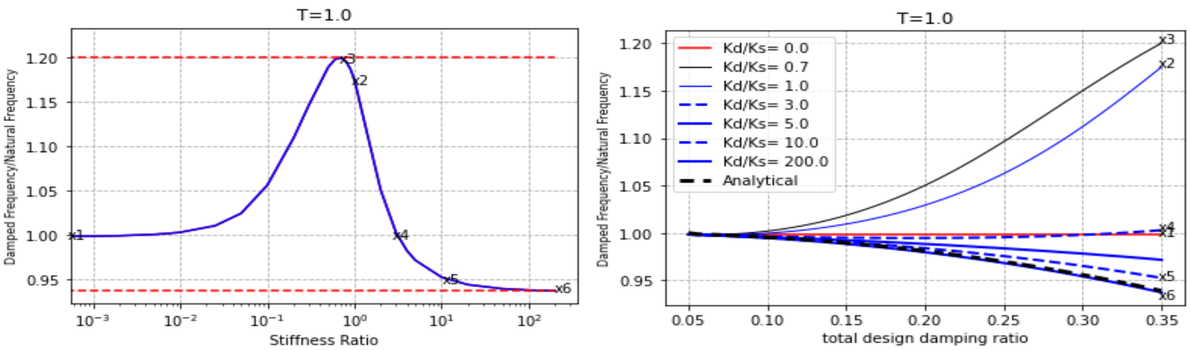

Figure(2) ωd/ωn values for T=1.0sec

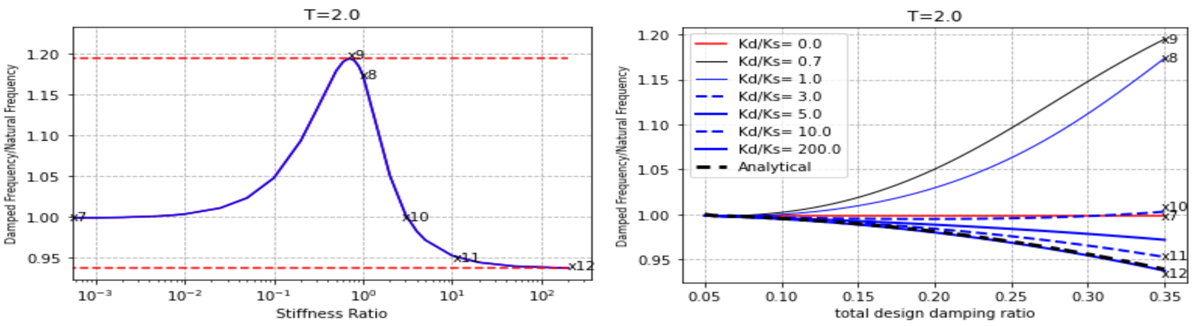

Figure(3)ωd/ωn values for T=2.0sec

The damped frequency drops relative to the natural frequency as the stiffness ratio exceeds three. The rigid subsystem with a stiffness of SR=200, which comprises near rigid subsystems with stiffnesses of SR=5 and SR=10, exhibits a longer duration than the extremely flexible subsystem with SR<3, as illustrated in Figure (4). The analytical solution shows the same pattern of the stiffness of the rigid subsystem derived from OpenSEES for a stiffness ratio of 200. This can be attributed to an analytical solution being suitable solely for virtually rigid subsystems. The bracing effect is evident when subsystem stiffness is below three times the intrinsic subsystem stiffness. The critical stiffnesses Kd/Ks= 0.7, 3.0, and 5.0 provide a useful framework for examining how these ratios change the phase difference in the system subjected to sinusoidal and earthquake excitations.

2.2 System component responses are subjected to sinusoidal excitation.

In this investigation, A sinusoidal excitation subjected to three different SDOF setups, structural system (combined), damper subsystem (spring), and viscous damper (dashpot), are modelled in OpenSEES and shown in Figure (4). This was initially introduced by (Xie et al., 2022) to find the effect of damper subsystem stiffness on the phasing responses between viscous damper and structural system. The "structural system" comprises an elastic spring, inherent damping, and a subsystem consisting of supplemental damping and subsystem stiffness. The "damper subsystem" does not consider supplemental damping. Instead, the elastic spring of the damper subsystem is considered an elastic uniaxial material. In contrast, for the "viscous damper", the stiffness of the subsystem is not considered, and the supplemental damping is characterised as a viscous uniaxial material.

The simplified design damping ratio is assumed to be 20%, and the natural period of the system is 3 seconds. These three different setups are subjected to sinusoidal excitation protocol is applied for 8 seconds and then released to vibrate freely for 12 seconds (total duration of the excitation is 20 seconds). Normalise the responses of the three systems by using the structural system responses of the structural system. The results of the pulse excitation demonstrated the influence of damper subsystem flexibility on the viscous damper's phasing with respect to the structural responses.

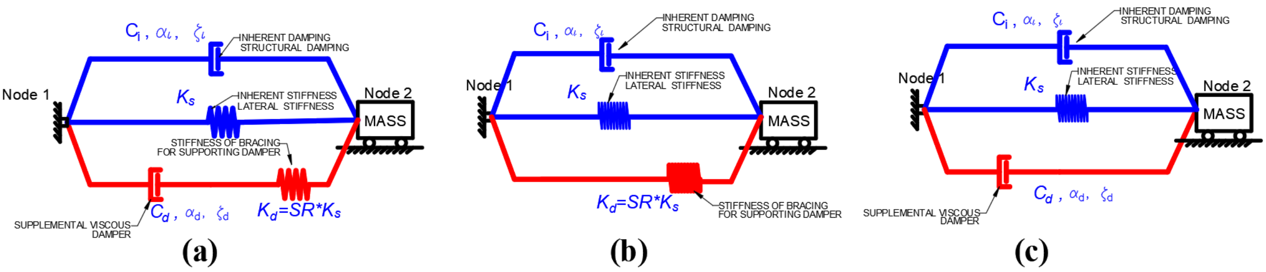

Figure (4) components of setups: a) structural system, b) damper subsystem, and c) viscous damper

Figure (5) demonstrates that the systems exhibited a distinct out-of-phase behaviour between the three systems in the highly flexible system (SR=0.7). The damper subsystem is dependent on the stiffness of the subsystem Kd, which exhibits greater oscillation than the viscous damper component. The viscous damper, on the other hand, can absorb some earthquake energy and experiences considerably less oscillation than the damper subsystem. It is noteworthy to observe that the oscillation of the structural system, considering both stiffness and supplemental damping, results in greater displacement compared to the viscous damper component. This is because a high flexibility of subsystems allows for more displacement.
When the stiffness ratio (SR) increases to 3.0, the systems exhibit a certain degree of in-phase behaviour between the structural system and the viscous damper. Additionally, the increase in stiffness aids the damper subsystem to decrease displacement effectively.

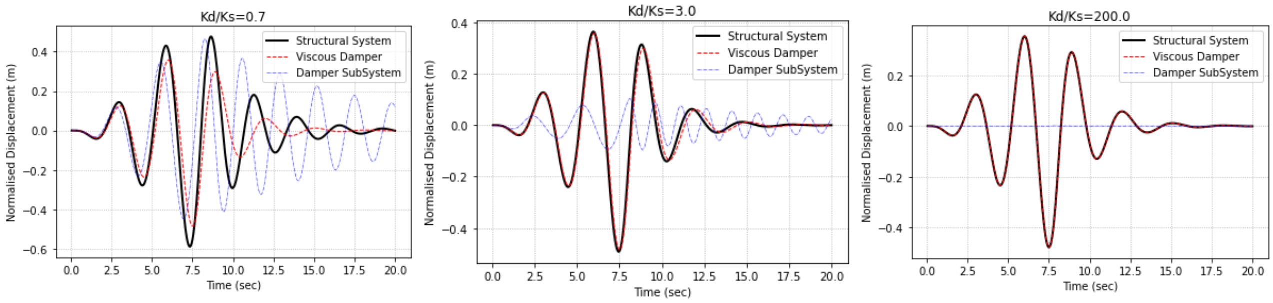

Figure(5) Normalised *time history displacement for Kd/Ks= 0.7, 3.0, and 200*

When the stiffness of the subsystem reaches a rigid level with a value of SR=200, the rigid subsystem experiences almost no displacement, leading to no movement in the damper subsystem. This observation is completely reversed with the damper subsystem (no viscous dashpot considered). The subsystem stiffness combines with the stiffness of the subsystem and then the overall system stops from movements.
Figure (6) visually demonstrates another instance of the flexibility phenomenon for these three systems under the same excitation protocol. The graphs depict the relationship between normalised displacement and damping force in the system. Results have been remarkably close to those expected specifically when the stiffness ratio (SR) is 0.7. This relationship is demonstrated by the damper subsystem-spring, which follows a linear pattern. When the stiffness of the subsystem grew to a stress ratio (SR) of 3.0, the displacement decreased by 40%. However, when the subsystem is rigid with an SR of 200, the damper subsystem does not oscillate. Nevertheless, the damping force remains unaffected by the stiffness of the damper subsystem combined.

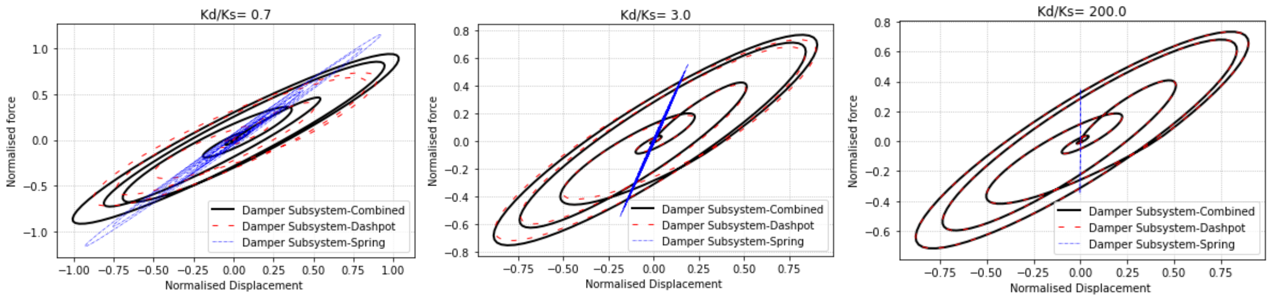

Figure (6) normalised displacement vs normalised force for Kd/Ks= 0.7, 3.0, and 200

It is unsurprising to find a considerable difference in the behaviour of the dashpot and the combined system, which is noticed in Figure (6). The supplementary viscous damper significantly influences the damping force in both the structural and viscous damper. However, these two components exhibit a phase difference with a low stiffness ratio (SR=0.7). Increasing the stiffness of the subsystem (SR=3.0) in the structural system is expected to result in a greater tendency towards in-phasing. A stiffness ratio of SR=0.7 demonstrates greater flexibility, enabling the structural system to lag the viscous damper. This can be verified using a rigid subsystem with a stiffness value of SR=200 when both systems display the same pattern.

It was found that such an observation produces expected results in the phasing responses of damper subsystem stiffness. As notified high flexible subsystem stiffness exhibit out-of-phase.

3 LINEAR VISCOUS DAMPER SUBSYSTEM STIFFNESS SUBJECTED TO EARTHQUAKE EXCITATION

This analytical observation is performed in OpenSEES to find the effect of brace flexibility on structural responses such as displacement and base shear subjected to earthquake excitation. Two different setups are proposed; the first system is an SDOF without a viscous damper comprised of linear spring Ks and viscous dashpot Ci, which is modelled to quantify $D_{5\%}$ (maximum displacement in the system with 5% inherent damping ratio). The second system is an SDOF system equipped with a viscous damper subsystem, including the linear spring Kd=SR*Ks and dashpot Cd to quantify D_{max} (maximum displacement in the system with designed damping ratio). A setup was developed in the PEER NGA platform to aid in scaling ground motion data and use them in time history analysis. the targeted response spectra curve for Christchurch is plotted based on (NZS 1170.5:2004) the assumed critical information of the soil Class D is assumed, and MCE is considered as occurrence probability is assumed to be 2% for 50 years. The site's range distance from the rapture is 0-100km". The hazard factor for Christchurch is proposed to be 0.4 (Gerstenberger et al., 2014). The mean response spectra of ground motions are scaled to the targeted response spectra before being used in time history analysis. In this observation, two SDOF systems are subjected to 20 earthquake ground motions to compute the maximum displacement and base shear reduction. An alternative configuration is the incorporation of a viscous damper, which includes a spring constant Kd and an additional viscous damping coefficient ζd=30%, into the single degree of freedom (SDOF) system.

3.1 DISPLACEMENT REDUCTION FACTOR

A unique pattern emerged from the OpenSEESpy time series analysis, a considerable decrease in structural responses was associated with an increase in the damper subsystem's stiffness ratio. In systems with high natural periods (Tn> 1 second), this effect was especially noticeable, proving that increasing stiffness effectively reduced dynamic responses ($D_{max}/D_{5\%}$ reduced approximately 45 to 55%).

Surprisingly, in systems with high-frequency systems (Tn=0.25 seconds), the stiffness of the subsystem has an inconsiderable effect on the structural reactions. This is because systems with short natural periods are nearly rigid and experience minimal displacement when subjected to strong seismic forces. In contrast, long-period systems undergo excessive displacement due to their high flexibility. In both cases, the combination of damping ratio and subsystem stiffness is obvious, whereas the effect of subsystem stiffness is more effective in long periods.

For structures with longer natural periods of high-rise buildings, for instance, the results indicate that considering the stiffness ratio of damper subsystems can be a useful strategy for further controlling and minimising structural responses such as displacement and base shear. Based on the unique properties of the viscous damper and the elastic spring properties associated with supporting brace, connection and cylindrical dashpots, these findings from the time history analysis offer beneficial suggestions for optimising the designs of the damper subsystem. Further examination of the notable finding in Figure (6) demonstrated that a stiffness ratio of 5% displayed an almost similar pattern to that of a nearly rigid subsystem's stiffness (SR=200). The pattern similarity implies that an SR= 5 may be seen as exceedingly advantageous, attaining similar outcomes to those achieved with a rigid subsystem.

3.2 BASE SHEAR REDUCTION- LINEAR VISCOUS DAMPER

Figure (7), illustrating the decrease in base shear as the stiffness of the viscous damper subsystem and supplemental damping ratios increase, exhibits a convincing pattern. Particularly, a higher damping coefficient is linked to a more significant decrease in base shear, and the graphs indicate that increasing the stiffness of the subsystem results in a more noticeable reduction in base shear

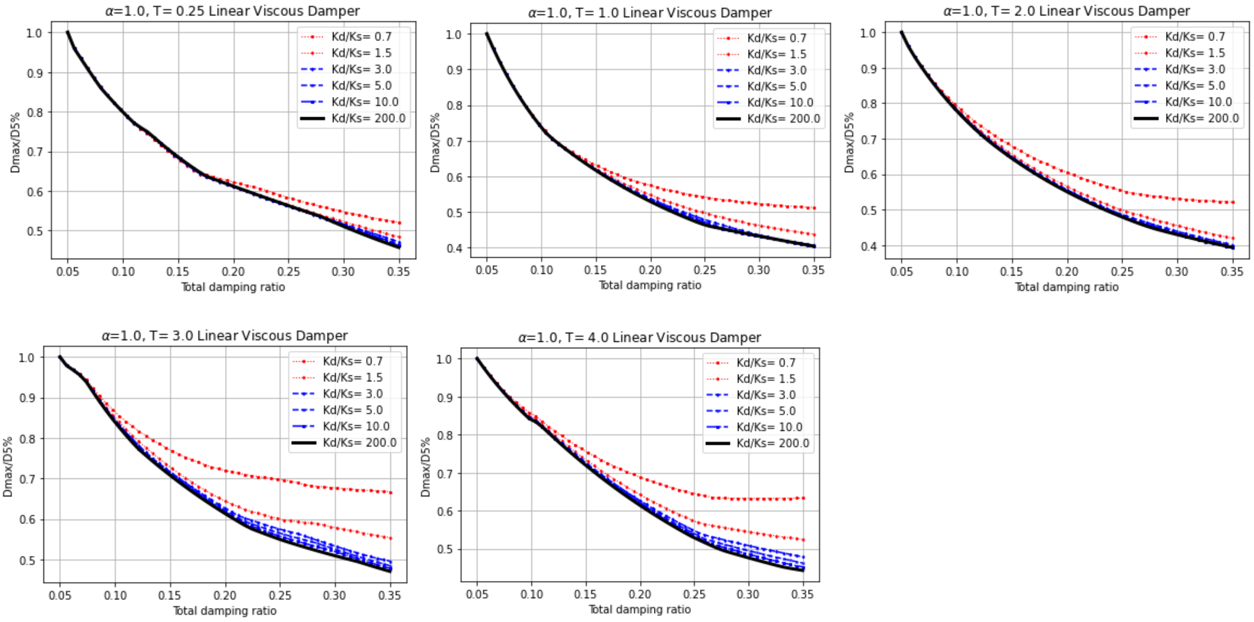

Figure (6) normalised displacement for T=0.25 ,1.0, 2.0, 3.0, and 4.0 seconds

. For the 0.25-second natural period of a system, having the same 50% of the designed damping ratio, the base shear reduction of SR=1 is almost close to SR=200 (45%). Furthermore, the reduction of base shear is noticeable for a system with a natural period of more than 1.0 seconds. The longer the natural period, the more pronounced the phenomena becomes. A notable finding arises when the decrease in the base shear reduction of the low stiffness subsystem becomes more apparent with the increase in the natural period. This demonstrates excellent agreement of the relation between base shear and velocity in sinusoidal excitation investigation when they are out of phase for low stiffness ratios. However, this is relatively adjusted by the rigid subsystem. This issue must be understood before designing the structure equipped with a supplemental damper to quantify the optimal amount of stiffness associated with a viscous damper.

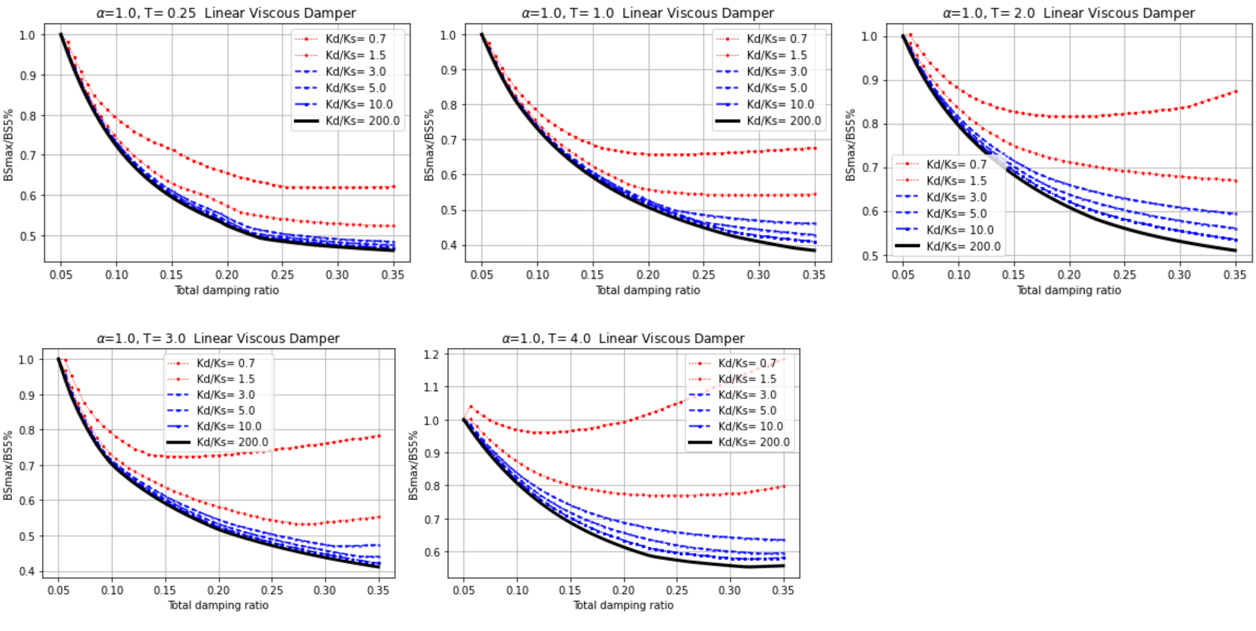

Figure (7) normalised base shear reduction for T=0.25 ,1.0, 2.0, 3.0, and 4.0 seconds

These observations highlight the importance of modifying the damper subsystem's stiffness to match the structure's specific characteristics. An optimal ratio of subsystem stiffness is achieved when the values 3.0 are reached in the all-natural time. The base shear reduction by SR=3 can be achieved as much as the reduction reached using SR=200. This has implications for improving earthquake resilience, especially in structures with high or low natural frequencies.

4 CONCLUSION:

The effect of damper subsystem stiffness on structural responses is investigated in three different excitations to quantify the optimal amount of stiffness ratio of the damper subsystem that effectively reduces structural responses. These three observations agree with Xie et al. (2022) which were similar to that investigated in this study. This study found that the optimal stiffness ratio is more likely higher than three. Base shear reduction is more effective with a highly flexible subsystem than displacement reduction. More research is needed to understand the impact of the damper stiffness on changing natural frequencies to avoid the resonance effect and the reduction in seismic energy.

REFERENCES

[Record #48 is using a reference type undefined in this output style.]

Abdi, H., Hejazi, F., Jaafar, M., & Karim, I. (2016). Evaluation of response modification factor for steel structures with soft story retrofitted by viscous damper device. *Advances in Structural Engineering*, *19*(8), 1275-1288.

Faruk, M. O., Singh, S., & Mondal, S. (2023). Comparative study of buckling restrained braces and fluid viscous damper applied in an RCC structure following pushover analysis. *Materials Today: Proceedings*.

Feng, H., Zhou, F., Ge, H., Zhu, H., & Zhou, L. (2021). Seismic performance enhancement of buildings using multi-limb brace damper systems. *The structural design of tall and special buildings*, *30*(3), e1825.

Gerstenberger, M., McVerry, G., Rhoades, D., & Stirling, M. (2014). Seismic hazard modeling for the recovery of Christchurch. *Earthquake Spectra*, *30*(1), 17-29.

Hejazi, F., Zabihi, A., & Jaafar, M. (2014). Development of elasto-plastic viscous damper finite element model for reinforced concrete frames. *Soil Dynamics and Earthquake Engineering*, *65*, 284-293.

Infanti, S., Robinson, J., & Smith, R. (2008). Viscous dampers for high-rise buildings. The 14th World Conference on Earthquake Engineering,

Kim, J., Choi, H., & Min, K.-W. (2003). Performance-based design of added viscous dampers using capacity spectrum method. *Journal of Earthquake Engineering*, *7*(01), 1-24.

Liu, Q., Li, P., Yuan, C., Li, W., & Ding, S. (2023). Experimental and analytical modelling on a novel self-centering viscous damper. *Journal of Building Engineering*, *75*, 107020.

Losanno, D., Hadad, H. A., & Serino, G. (2017). Seismic behavior of isolated bridges with additional damping under far-field and near fault ground motion. *Earthquakes and Structures*, *13*(2), 119-130.

Mansoori, M., & Moghadam, A. (2009). Using viscous damper distribution to reduce multiple seismic responses of asymmetric structures. *Journal of Constructional Steel Research*, *65*(12), 2176-2185.

Mcnamara, R. J., & Taylor, D. P. (2003). Fluid viscous dampers for high-rise buildings. *The structural design of tall and special buildings*, *12*(2), 145-154.

NEHRP. (2001). *NEHRP Recommended Provisions (National Earthquake Hazards Reduction Program) for Seismic Regulations for New Buildings and Other Structures*. Building Seismic Safety Council.

Oinam, R. M., Sahoo, D. R., & Sindhu, R. (2014). Cyclic response of non-ductile RC frame with steel fibers at beam-column joints and plastic hinge regions. *Journal of Earthquake Engineering*, *18*(6), 908-928.

Patel, C., & Jangid, R. (2014). Dynamic response of identical adjacent structures connected by viscous damper. *Structural Control and Health Monitoring*, *21*(2), 205-224.

Pourzangbar, A., Vaezi, M., Mousavi, S., & Saber, A. (2020). Effects of brace-viscous damper system on the dynamic response of steel frames. *International Journal of Engineering*, *33*(5), 720-731.

Sabelli, R. (2001). *Research on improving the design and analysis of earthquake-resistant steel-braced frames*. EERI Oakland, CA, USA.
Seo, C. Y., Karavasilis, T. L., Ricles, J. M., & Sause, R. (2014). Seismic performance and probabilistic collapse resistance assessment of steel moment resisting frames with fluid viscous dampers. *Earthquake Engineering & Structural Dynamics*, *43*(14), 2135-2154.
Silwal, B., Michael, R. J., & Ozbulut, O. E. (2015). A superelastic viscous damper for enhanced seismic performance of steel moment frames. *Engineering Structures*, *105*, 152-164.
Symans, M. D., Charney, F. A., Whittaker, A., Constantinou, M. C., Kircher, C., Johnson, M. W., & McNamara, R. J. (2008). Energy dissipation systems for seismic applications: current practice and recent developments. *Journal of Structural Engineering*, *134*(1), 3-21.
Xie, R., Rodgers, G., & Sullivan, T. (2022). Effect of damper sub-system stiffness on the response of a single degree of freedom system equipped with a viscous damper. *Journal of Earthquake Engineering*, *26*(11), 5907-5926.
Zhang, W., Zhang, C., Su, L., Zheng, Y., & Du, X. (2023). Experimental study on the dynamic performance of a winding rope fluid viscous damper. *Engineering Structures*, *281*, 115786.
ZHU, L.-h., WANG, J., YU, A.-q., & SHAN, S.-y. (2019). A novel viscous damper installation configuration considering architectural requirements. *Engineering Mechanics*, *36*(8), 210-216,225.